

# Two-Dimensional Skyrmion Lattice Formation in a Nematic Liquid Crystal Consisting of Highly Bent Banana Molecules

Sungmin Kang,\* Eun-Woo Lee, Tianqi Li, Xiaobin Liang, Masatoshi Tokita, Ken Nakajima, and Junji Watanabe

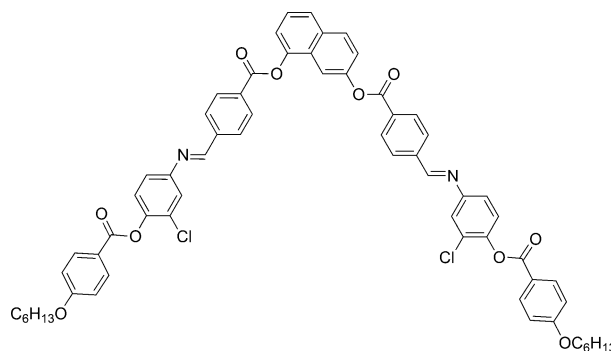
**Abstract:** We synthesized a novel banana-shaped molecule based on a 1,7-naphthalene central core that exhibits a distinct mesomorphism of the nematic-to-nematic phase transition. Both the X-ray profile and direct imaging of atomic force microscopy (AFM) investigations clearly indicates the formation of an anomalous nematic phase possessing a two-dimensional (2D) tetragonal lattice with a large edge (ca. 59 Å) directed perpendicular to the director in the low-temperature nematic phase. One plausible model is proposed by an analogy of skyrmion lattice in which two types of cylinders formed from left- and right-handed twist-bend helices stack into a 2D tetragonal lattice, diminishing the inversion domain wall.

The geometrical features of liquid-crystalline (LC) molecules largely decide the form of LC phases. For example, rod-like molecules exhibit calamitic phases of nematic (N) and smectic (Sm), whereas disc- and lath-like molecules exhibit discotic columnar (Col<sub>D</sub>) and discotic nematic (N<sub>D</sub>) phases, respectively. Among the LCs, bent-core liquid crystals (BCLC) have attracted considerable attention because they spontaneously form chirality and polarity from achiral molecules, resulting in unique banana (B) phases, for example, various Sm sub-phases constructed as an intercalation or a frustration in two-dimensional (2D) planes.<sup>[1]</sup> Thus, the overall molecular shape is thought to largely determine the mesomorphism. The shape of BCLC can be effectively designed by controlling the opening angle (OA) of the central core moiety in a molecular Scheme. The OA that favors the banana phases has been reported as below 140°. <sup>[2]</sup> The mesomorphism of BCLC with smaller bent angles (< 90°), the so-called “low bent-angle BCLCs”, are apparently less developed, despite several early reports describing the formation of calamitic LCs.<sup>[3]</sup> However, we recently found that low bent-angle derivatives with OA of 60° can form representative B phases of B<sub>2</sub>, B<sub>4</sub>, B<sub>7</sub>, and a polar SmA phases.<sup>[4]</sup> Furthermore, by combining with long alkylsulfanyl chains, they can form not only a novel switchable hexagonal columnar phase but also an optically isotropic phase with a cubic lattice.<sup>[5]</sup> Notably, the formation of polar B phases

provides overriding evidence that in these systems, molecules can pack along the bent direction despite the small OA of 60°.

In typical BCLC with bent angles around 120°, the N phase is replaced by the B<sub>6</sub> phase, an intercalated layered structure.<sup>[6]</sup> On the other hand, the N phase becomes dominant with larger OA (> 120°)<sup>[2]</sup> or significant asymmetry in their schemes, such as hockey-stick-shaped LCs.<sup>[7]</sup>

Among the above formations, the N phase formed by low bent-angle BCLC is notable because the direction of the *n*-director is an additional concern (parallel or perpendicular to the bent (*b*) direction). When the *b* direction is lying along the *n*-director, they are known to form calamitic LCs similar to rod-like LCs.<sup>[3]</sup> In contrast, the perpendicular orientation of the *b* direction to the *n*-director is relatively rare. We have reported that this arrangement can potentially form B phases by adopting a seven-membered ring system with a 1,7-naphthalene core.<sup>[4a]</sup> As part of our investigations on an ultimate structure-LC property, we have prepared a novel low bent-angle (highly bent) BCLC based on a 1,7-naphthalene core, 1Cl-N(1,7)-O6, which exhibits curious N phases. 1Cl-N(1,7)-O6 comprises two side wings, each composed of three aromatic rings with a lateral chlorine substitution and alkoxy tails with 6-carbon numbers (Scheme 1 and S1 in the Supporting Information).<sup>[8]</sup>



**Scheme 1.** Chemical structure of 1Cl-N(1,7)-O6.

The phase sequential behavior obtained by differential scanning calorimetry (DSC) upon heating and cooling at a scanning rate of 10 °C min<sup>-1</sup>, are presented in Figure 1 and Table 1. In Figure 1, two peaks appear at 178 °C and 212 °C on heating and at 211 °C and 162 °C on cooling. Polarizing optical microscopy (POM) observations revealed an isotropic (Iso)-N phase transition. Upon cooling from the Iso, a typical schlieren texture with two- and four-brush point singularities appeared under cross-nicol, which flashed under mechanical

[\*] Prof. Dr. S. Kang, Dr. E.-W. Lee, T. Li, Prof. Dr. X. Liang, Prof. Dr. M. Tokita, Prof. Dr. K. Nakajima, Prof. Dr. J. Watanabe  
Department of Chemical Science and Engineering  
School of Materials and Chemical Technology  
Tokyo Institute of Technology  
2-12-1 O-okayama, Tokyo 152-8552 (Japan)  
E-mail: skang@polymer.titech.ac.jp

Supporting information and the ORCID identification number(s) for the author(s) of this article can be found under <http://dx.doi.org/10.1002/anie.201606388>.

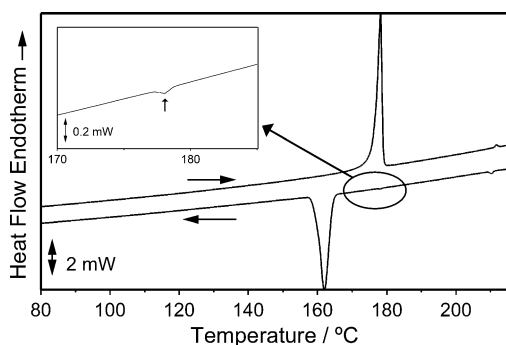


**Figure 1.** DSC thermogram for 1Cl-N(1,7)-O6 (inset: enlargement of the N1–N2 phase transition).

**Table 1:** Phase transition behaviors.

Process	Transition property [Temperature ( <i>Enthalpy</i> ): °C (kJ mol <sup>−1</sup> )]
Cooling	Cr 162(37.2) N2 178(0.07) N1 211(0.30) Iso
Heating	Cr 178(38.0) N1 212(0.29) Iso

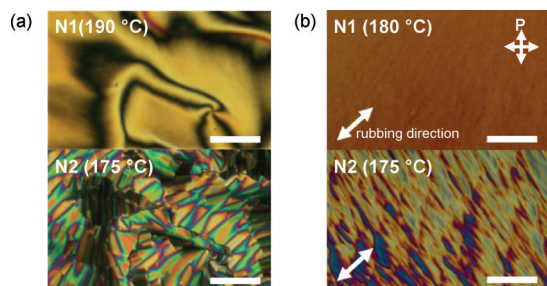


**Figure 2.** Polarized optical microscope images of N1 and N2 phase with different sample preparations. a) unrubbed planar alignment and b) rubbed homogeneous cells. Cell thickness: 5  $\mu\text{m}$ .

stress (Figure 2a). In addition, a well-developed uniform texture was observed in the rubbed cell (Figure 2b). These features, along with the well-defined response to external electric and magnetic fields ( $B$ ; see below), are reminiscent of a N phase.

Careful observation of the DSC thermogram reveals an additional exothermic peak at 178 °C during the cooling process (Figure 1, inset). The low-temperature LC phase then becomes obvious, but is monotropic as it exists in the temperature region 178–162 °C. The enthalpy change between the two phases is negligibly small (0.07 kJ mol<sup>−1</sup>), indicating the high similarity of the LC structures. This transition, however, induced remarkable textural changes in the polarized optical microscope (POM) images. Upon entering the low-temperature phase below 178 °C, the schlieren and uniform texture (Figure 2top) transformed into a fan-like texture (Figure 2bottom), respectively. Interestingly, the longitudinal edge (usually it indicates a direction of 1D ordering) of the fan-like domain was perpendicular to the  $n$ -director in the preceding high-temperature N phase, as observed in Figure 2 and S1 (for shear aligned sample and

optical properties). Thus, we tentatively named the high- and low-temperature N phases as N1 and N2, respectively. Upon electro-optical measurements, the dielectric response of the Fredericks transition was confirmed (Figure S2, S3). No polar switching behavior (up to 16 V  $\mu\text{m}^{-1}$ ) was detected in both phases.

The details of the structure were clarified by wide angle X-ray diffraction (WAXD) and small angle X-ray scattering (SAXS). Figure 3 shows the oriented 2D WAXD profiles of

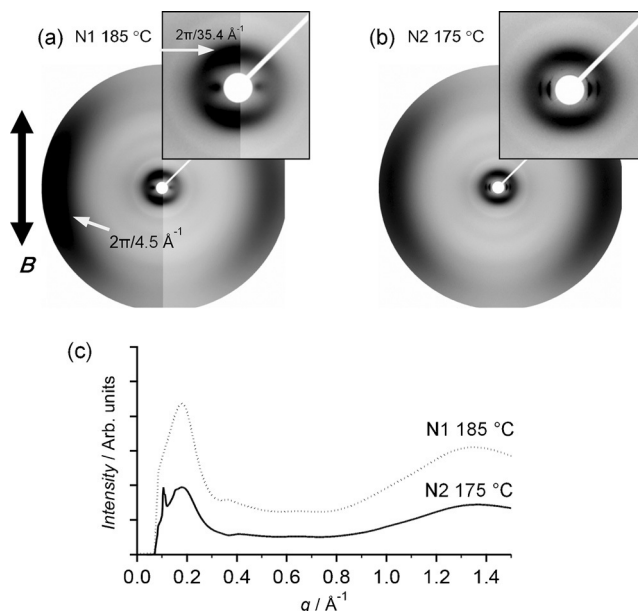


**Figure 3.** a,b) Oriented 2D and c) 1D profiles of the WAXD measurement. (insets: enlargements of small angle region).

both phases under  $B$  (ca. 1 T) during cooling from Iso. There are two characteristic broad scatterings at  $q$  ( $=2\pi/d$ )  $= 2\pi/4.5 \text{ Å}^{-1}$  on the equator and  $q = 2\pi/35.4 \text{ Å}^{-1}$  in the meridional line. From these results, we immediately deduce that no long-range positional order exists along the  $n$ -director, implying a nematic nature (Figure 3c). Thus, the 35.4 Å spacing obtained from the inner diffuse scattering can be interpreted as the average molecular length (ML) along the director.<sup>[4a]</sup>

The profile differences between the N1 and N2 phases are more obvious in the oriented SAXS profiles (Figure 4). In both phases, the scatterings on the equator are prominent,

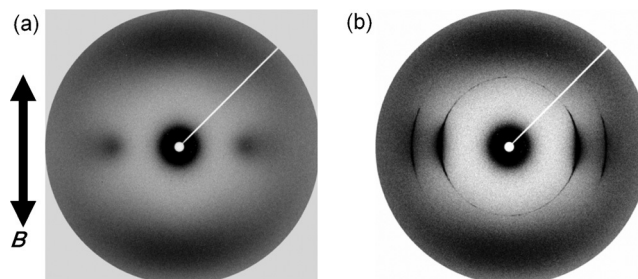


**Figure 4.** Oriented 2D profiles of the SAXS measurement a) N1 and b) N2 phases.

which are perpendicular to the  $n$ -director ( $B$  direction) in addition to the diffuse halo appearing on the meridional line at  $q = 2\pi/35.4 \text{ \AA}^{-1}$ . In the N1, the profile appears as halos at  $q = 2\pi/57.0 \text{ \AA}^{-1}$ , whereas cooling to the N2 yields clear reflections at  $q = 2\pi/59.0 \text{ \AA}^{-1}$  and  $2\pi/41.0 \text{ \AA}^{-1}$ . These two reflections can be indexed as  $(100)$  and  $(110)$ , respectively, assuming a tetragonal lattice with one edge,  $a = 59.0 \text{ \AA}$ . As a result, the N2 phase is interpretable as a nematic phase with a definite electron density wave of  $59.0 \text{ \AA}$  perpendicular to the  $n$ -director, whereas the N1 exhibits a more modest average density wave of  $57.0 \text{ \AA}$ . The size and tetragonal symmetry are unaffected within the range of N1 and N2. The tetragonal symmetry is also revealed by WAXD and SAXS with a planar-oriented sample, indicating four orthogonal spot-like reflections (Figure S4). These results indicate that the transition from N1 to N2 is followed by a disorder–order transition of the 2D tetragonal lattice. Assuming a density of  $1.0\text{--}1.2 \text{ g cm}^{-3}$ , lattice parameter  $a = 59.0 \text{ \AA}$  and a molecular height  $h = 35.4 \text{ \AA}$  along the director, there are 67–80 molecules in each 2D tetragonal lattice unit.

A tetragonal lattice can be imagined as a discotic columnar assembly formed by columnar-stacked aromatic parts surrounded by aliphatic chains, which will lead an orthogonal arrangement between the molecules and column axis. However, such arrangements are unlikely in this case since the molecule and column axis align parallel each other (The molecular director is perpendicular to the 2D lattice plane). Furthermore, a Col<sub>p</sub> is unlikely to adopt a tetragonal packing symmetry considering the closest packing. Also, the isotropization enthalpy of the present phase is  $0.3 \text{ kJ mol}^{-1}$ , much smaller than  $5\text{--}7 \text{ kJ mol}^{-1}$  for previous reports of Col phases.

The above results raise two questions. First, can a 2D lattice perpendicular to the director emerge from the continuum nematic fluid LC? Second, why is the packing symmetry tetragonal rather than hexagonal? A satisfactory candidate demands that the system is chiral and includes a 2D array of topological defects, as typically observed in blue phases (BP).

Recently, a twist-bend (TB) nematic ( $N_{TB}$ ) phase has been structurally characterized.<sup>[9]</sup> In this phase, achiral molecules in a unique nematic ground state order into a layer-free, heliconal LC of nanoscale pitch. The  $N_{TB}$  phase was theoretically predicted<sup>[10]</sup> and suggested that the local bend curvature in the director field of bent-shaped molecules could stabilize the twist and bend director distributions, with the molecules recessing on a cone (Figure 5a,b).<sup>[11]</sup> The nematic features, spontaneous chirality<sup>[12]</sup> and fan-like textures<sup>[13]</sup> of this phase (but lack of Sm-like layer X-ray diffraction peaks<sup>[9c]</sup>) have been interpreted in terms of the  $N_{TB}$  structure. The helix periodicity was reported as approximately 8–14 nm.<sup>[14]</sup> Moreover, the low bend elastic constant<sup>[15]</sup> and two optically opposite, large chiral domain phases were reported.<sup>[9a]</sup>

However, if the domain size reduces below a certain size, the 1D structure might be less stable than 2D or 3D structures. This destabilization would depend on the boundary conditions. In other words, double-helix cylinders may assemble into phases with strong defect density, similar to the blue

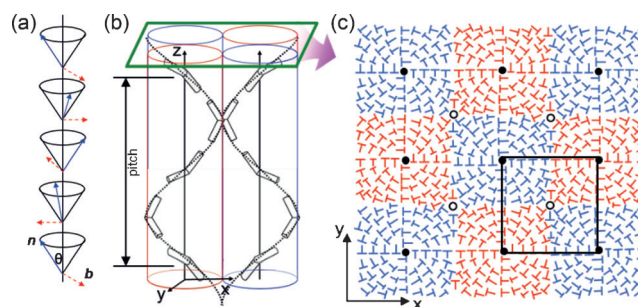


**Figure 5.** Schematic illustrations of a) conical local director distributions of  $n$ - and bend  $b$ -directors. b) a twist-bend director distribution alike  $N_{TB}$  phase forming right-handed (blue) and left-handed (red) helical ordering and c) a possible image of molecular projection and skyrmion-type 2D tetragonal lattice model based on cylindrical arrays by neighboring opposite helicity. See text for details.

phase (BP),<sup>[16]</sup> characterized by 3D ordering of the director, which denotes the average orientation of the LC molecules. The local preference for a double-twist structure over a single-twist in the helical phase is delicately balanced against the global topological constraint that prevents a double-twist structure from filling the whole space with no discontinuities. This balance leads to 3D regular stacking of so-called double-twist cylinder (DTC) and topological defect lines.<sup>[16]</sup> DTCs exhibit a  $\pi/4$  rotation of the directors from the center in all directions perpendicular to the cylinder; consequently, the  $n$ -director field in BP remains continuous at the contact points between two neighboring orthogonal DTC.

More recently, the  $\pi/4$  rotation of DTC has been argued as a type of skyrmion excitation.<sup>[17]</sup> Skyrmions, particle-like topological entities in a continuum field, play an important role in various condensed matters.<sup>[18]</sup> It was confirmed that a highly chiral NLC accommodating a quasi-2D skyrmion lattice is thermodynamically stable when confined to a thin film between two parallel surfaces.<sup>[19]</sup> Skyrmion lattice ground states may exist in bulk compounds as well as at surfaces and in thin films.<sup>[20]</sup>

Let us return to the present system. Figure 5c illustrates a projection of molecules and a possible skyrmion-type 2D tetragonal lattice, based on the conical twist-bend helix model. Defect lines with  $s = +1$  (Figure 5c solid dot) and  $s = -1$  (Figure 5c empty dot) reside at the centers and boundaries of the cylindrical arrays. The right- and left-handed cylinders regularly alternate in a 2D lattice with tetragonal symmetry. In this way, the cylinders are embedded in a regular lattice of topological defects. The red and blue nails in Figure 5c indicate the handedness of helices. Because the nails are vectorial, skyrmions with positive chirality must neighbor those with negative; otherwise, the boundary between two skyrmions would be discontinuous. Therefore, a hexagonal symmetry is restricted because it would lead to frustrations with the inversion domain walls. In contrast, continuum director fields are allowed in the tetragonal symmetry, forming disclinations of  $s = -1$ . In other words, chiral interactions prevent a space inversion symmetry. In fact, such a 2D skyrmion lattice with tetragonal symmetry was reported for the ground state of magnetic metals.<sup>[20]</sup> Similar



chiral cylinders might exist in the high-temperature N1 phase, but the disorder-order transition followed by the negligibly small transition enthalpy leads to random placement of the declinations.

The direction of bent axis in the nematic field is not fully confirmed. However, the averaged ML observed by X-ray, 35.4 Å, is satisfactory for the model in Figure 5 since the end-to-end distance between two terminal carbons can meet the value<sup>[21]</sup> (Figure S5) while the maximum length of the longer sidearm remains under 32.7 Å which cannot meet the ML value. It should be also noted that the molecular orientation (bent direction) in Figure 5b is not an absolute requirement for the formation of tetragonal structure. If a molecular packing with the bent axis along the *n*-director satisfies above mentioned conditions for the tetragonal lattice, it can also be a possible candidate until more solid information about their alignments is obtained.

Finally, a surface morphology of LC film was investigated by atomic force microscopy (AFM), and a direct imaging of the tetragonal order (ca. 60 Å) was successfully achieved. Figure 6 and Figure S6 clearly show well-defined stripe patterns with a periodicity of around 60 Å lying along the shear direction; moreover, the periodicity lies in a direction perpendicular to the shear direction, which is consistent with the polarized optical microscope images (Figure 2, S1).

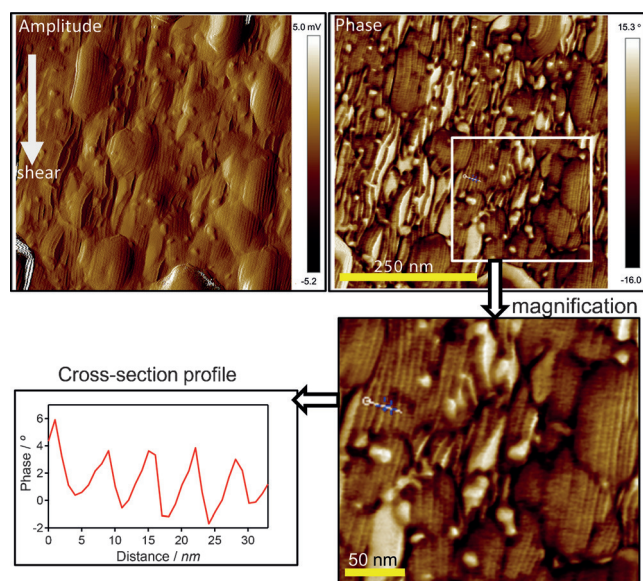


**Figure 6.** AFM images obtained for the N2 phase film surface. Clear stripe lines with a periodicity of approximately 60 Å were detected lying along the shear direction.

In summary, two nematic phases of a novel acute-angle BCLC were extensively examined by X-ray and AFM investigations. The result provides clear evidence of a novel tetragonal lattice order in the low-temperature N2, and its pre-translational pseudo-tetragonal structure in the high-temperature N1 phase. The mesomorphic transition behavior between the N1 and the N2 phases can be understood as a disorder–order transition, in which a frustrated structure

with a 2D tetragonal lattice might be stabilized by chiral interactions between the right-handed and left-handed cylinders, precluding a space inversion symmetry. This result exemplifies a crucial step in discovering novel molecular assemblies in BCLC systems, improving our understanding of structure–property relationships and offering opportunities for their control.

## Acknowledgements

This research was supported by a Grant-in-Aid for Scientific Research (c) from the Ministry of Education, Culture, Sports, Science and Technology in Japan (26410086). The SR X-ray measurement was performed at the 4C beamline in the Pohang Light Source II.

**Keywords:** bent-shaped molecule · liquid crystals · nematic phase · phase transition · tetragonal symmetry

**How to cite:** *Angew. Chem. Int. Ed.* **2016**, *55*, 11552–11556  
*Angew. Chem.* **2016**, *128*, 11724–11728

- [1] a) T. Niori, T. Sekine, J. Watanabe, T. Furukawa, H. Takezoe, *J. Mater. Chem.* **1996**, *6*, 1231–1233; b) D. R. Link, G. Natale, R. Shao, J. E. MacLennan, N. A. Clark, E. Körblova, D. M. Walba, *Science* **1997**, *278*, 1924–1927; c) J. Watanabe, T. Niori, T. Sekine, H. Takezoe, *Jpn. J. Appl. Phys. Part 2* **1998**, *37*, L139–L142; d) G. Pelzl, S. Diele, W. Weissflog, *Adv. Mater.* **1999**, *11*, 707–724; e) J. Thisayukta, H. Takezoe, J. Watanabe, *Jpn. J. Appl. Phys.* **2001**, *40*, 3277–3287; f) D. A. Coleman, J. Fernsler, N. Chattham, M. Nakata, Y. Takanishi, E. Körblova, D. R. Link, R.-F. Shao, W. G. Jang, J. E. MacLennan, O. Mondainn-Monval, C. Boyer, W. Weissflog, G. Pelzl, L. C. Chien, J. Zasadzinski, J. Watanabe, D. M. Walba, H. Takezoe, N. A. Clark, *Science* **2003**, *301*, 1204–1211; g) R. A. Reddy, C. Tschierske, *J. Mater. Chem.* **2006**, *16*, 907–961.
- [2] a) G. Pelzl, S. Diele, S. Grande, A. Jákli, CH. Lischka, H. Kresse, H. Schmalfuss, I. Wirth, W. Weissflog, *Liq. Cryst.* **1999**, *26*, 401–413; b) W. Weissflog, H. Nádasi, U. Dunemann, G. Pelzl, S. Diele, A. Eremin, H. Kresse, *J. Mater. Chem.* **2001**, *11*, 2748–2758; c) S. Kang, Y. Saito, N. Watanabe, M. Tokita, Y. Takanishi, H. Takezoe, J. Watanabe, *J. Phys. Chem. B* **2006**, *110*, 5205–5214; d) C. V. Yelamagad, M. Mathews, S. A. Nagamani, D. S. S. Rao, S. K. Prasad, S. Findeisen, W. Weissflog, *J. Mater. Chem.* **2007**, *17*, 284–298.
- [3] a) H. Matsuzaki, Y. Matsunaga, *Liq. Cryst.* **1993**, *14*, 105–120; b) M. Kuboshita, Y. Matsunaga, H. Matsuzaki, *Mol. Cryst. Liq. Cryst.* **1991**, *199*, 319–326; c) C. V. Yelamagad, I. Shashikala, D. S. S. Rao, S. K. Prasad, *Liq. Cryst.* **2004**, *31*, 1027–1036.
- [4] a) S. K. Lee, X. Li, S. Kang, M. Tokita, J. Watanabe, *J. Mater. Chem.* **2009**, *19*, 4517–4522; b) X. Li, S. K. Lee, S. Kang, M. Tokita, S. Kawauchi, J. Watanabe, *Chem. Lett.* **2009**, *38*, 424–425; c) E.-W. Lee, K. Takimoto, M. Tokita, J. Watanabe, S. Kang, *Angew. Chem. Int. Ed.* **2014**, *53*, 8216–8220; *Angew. Chem.* **2014**, *126*, 8355–8359.
- [5] a) X. Li, S. Kang, S. K. Lee, M. Tokita, J. Watanabe, *Jpn. J. Appl. Phys.* **2010**, *49*, 121701; b) S. Kang, M. Harada, X. Li, M. Tokita, J. Watanabe, *Soft Matter* **2012**, *8*, 1916–1922; c) E.-W. Lee, M. Hattori, F. Uehara, M. Tokita, S. Kawauchi, J. Watanabe, S. Kang, *J. Mater. Chem. C* **2015**, *3*, 2266–2273.
- [6] a) D. Shen, S. Diele, G. Pelzl, I. Wirth, C. Tschierske, *J. Mater. Chem.* **1999**, *9*, 661–672; b) G. Pelzl, I. Wirth, W. Weissflog, *Liq. Cryst.* **2001**, *28*, 969–972; c) W. Weissflog, I. Wirth, S. Diele, G.

- Pelzl, H. Schmalfuss, T. Schoss, A. Würflinger, *Liq. Cryst.* **2001**, *28*, 1603–1609; d) J. C. Rouillon, J. P. Marcerou, M. Laguerre, H. T. Nguyen, M. F. Achard, *J. Mater. Chem.* **2001**, *11*, 2946–2950; e) S. Kang, S. K. Lee, M. Tokita, J. Watanabe, *Phys. Rev. E* **2009**, *80*, 042703.
- [7] a) J. Matraszek, J. Mieczkowski, J. Szydłowska, E. Gorecka, *Liq. Cryst.* **2000**, *27*, 429–436; b) I. Wirth, S. Diele, A. Eremin, G. Pelzl, S. Grande, L. Kovalenko, N. Pancenko, W. Weissflog, *J. Mater. Chem.* **2001**, *11*, 1642–1650; c) S. I. Torgova, L. A. Karamysheva, T. A. Geivandova, A. Strigazzi, *Mol. Cryst. Liq. Cryst.* **2001**, *365*, 99–106; d) M. W. Schröder, S. Diele, G. Pelzl, U. Dunemann, H. Kresse, W. Weissflog, *J. Mater. Chem.* **2003**, *13*, 1877–1882; e) V. Prasad, S.-W. Kang, K. A. Suresh, L. Joshi, Q. Wang, S. Kumar, *J. Am. Chem. Soc.* **2005**, *127*, 17224–17227; f) R. Stannarius, J. Heuer, *Eur. Phys. J. E* **2007**, *24*, 27–33; g) C. Keith, A. Lehmann, U. Baumeister, M. Prehm, C. Tschierske, *Soft Matter* **2010**, *6*, 1704–1721.
- [8] a) S. K. Lee, Y. Naito, L. Shi, M. Tokita, H. Takezoe, J. Watanabe, *Liq. Cryst.* **2007**, *34*, 935–943; b) S. K. Lee, L. Shi, R. Ishige, S. Kang, M. Tokita, J. Watanabe, *Chem. Lett.* **2008**, *37*, 1230–1231.
- [9] a) G. Pelzl, A. Eremin, S. Diele, H. Kresse, W. Weissflog, *J. Mater. Chem.* **2002**, *12*, 2591–2593; b) P. J. Barnes, A. G. Douglass, S. K. Heeks, G. R. Luckhurst, *Liq. Cryst.* **1993**, *13*, 603–613; c) C. T. Imrie, P. A. Henderson, *Chem. Soc. Rev.* **2007**, *36*, 2096–2124; d) V. P. Panov, M. Nagaraj, J. K. Vij, Yu. P. Panarin, A. Kohlmeier, M. G. Tamba, R. A. Lewis, G. H. Mehl, *Phys. Rev. Lett.* **2010**, *105*, 167801; e) M. Cestari, S. Diez-Berart, D. A. Dunmur, A. Ferrarini, M. R. de la Fuente, D. J. B. Jackson, D. O. Lopez, G. R. Luckhurst, M. A. Perez-Jubindo, R. M. Richardson, J. Salud, B. A. Timimi, H. Zimmermann, *Phys. Rev. E* **2011**, *84*, 031704.
- [10] R. B. Meyer, in *Molecular Fluids, Vol. XXV-1973 of Les Houches Summer School in Theoretical Physics* (Eds.: R. Balian, G. Weill), Gordon and Breach, New York, **1976**, pp. 273–373.
- [11] a) I. Dozov, *Europhys. Lett.* **2001**, *56*, 247–253; b) R. Memmer, *Liq. Cryst.* **2002**, *29*, 483–496.
- [12] a) L. Beguin, J. W. Emsley, M. Lelli, A. Lesage, G. R. Luckhurst, B. A. Timimi, H. Zimmermann, *J. Phys. Chem. B* **2012**, *116*, 7940–7951; b) V. P. Panov, R. Balachandran, J. K. Vij, M. G. Tamba, A. Kohlmeier, G. H. Mehl, *Appl. Phys. Lett.* **2012**, *101*, 234106.
- [13] a) P. A. Henderson, C. T. Imrie, *Liq. Cryst.* **2011**, *38*, 1407–1414; b) M. G. Tamba, U. Baumeister, G. Pelzl, W. Weissflog, *Liq. Cryst.* **2010**, *37*, 853; c) K. Adlem, M. Čopič, G. R. Luckhurst, A. Mertelj, O. Parri, R. M. Richardson, B. D. Snow, B. A. Timimi, R. P. Tuffin, D. Wilkes, *Phys. Rev. E* **2013**, *88*, 022503.
- [14] a) D. Chen, J. H. Porada, J. B. Hooper, A. Klittnick, Y. Shen, M. R. Tuchband, E. Korblova, D. Bedrov, D. M. Walba, M. A. Glaser, J. E. MacLennan, N. A. Clark, *Proc. Natl. Acad. Sci. USA* **2013**, *110*, 15931–15936; b) V. Borschch, Y.-K. Kim, J. Xiang, M. Gao, A. Jákli, V. P. Panov, J. K. Vij, C. T. Imrie, M. G. Tamba, G. H. Mehl, O. D. Lavrentovich, *Nat. Commun.* **2013**, *4*, 2635; c) D. Chen, M. Nakata, R. Shao, M. R. Tuchband, M. Shuai, U. Baumeister, W. Weissflog, D. M. Walba, M. A. Glaser, J. E. MacLennan, N. A. Clark, *Phys. Rev. E* **2014**, *89*, 022566.
- [15] a) S. Kaur, L. Tian, H. Liu, C. Greco, A. Ferrarini, J. Seltmann, M. Lehmann, H. F. Gleeson, *J. Mater. Chem. C* **2013**, *1*, 2416–2425; b) S. Kaur, H. Liu, J. Addis, C. Greco, A. Ferrarini, V. Görtz, J. W. Goodby, H. F. Gleeson, *J. Mater. Chem. C* **2013**, *1*, 6667–6676.
- [16] D. C. Wright, N. D. Mermin, *Rev. Mod. Phys.* **1989**, *61*, 385–432.
- [17] a) B. Binz, A. Vishwanath, V. Aji, *Phys. Rev. Lett.* **2006**, *96*, 207202; b) S. Mühlbauer, B. Binz, F. Jonietz, C. Pfleiderer, A. Rosch, A. Neubauer, R. Georgii, P. Böni, *Science* **2009**, *323*, 915–919; c) S. Tewari, D. Belitz, T. R. Kirkpatrick, *Phys. Rev. Lett.* **2006**, *96*, 042703; d) I. Fischer, N. Shah, A. Rosch, *Phys. Rev. B* **2008**, *77*, 024415.
- [18] a) T. Skyrme, *Nucl. Phys.* **1962**, *31*, 556–569; b) L. Brey, H. A. Fertig, R. Côté, A. H. MacDonald, *Phys. Rev. Lett.* **1995**, *75*, 2562–2565; c) A. Schmeller, J. P. Eisenstein, L. N. Pfeiffer, K. W. West, *Phys. Rev. Lett.* **1995**, *75*, 4290–4293; d) A. Neubauer, C. Pfleiderer, B. Binz, A. Rosch, R. Ritz, P. G. Niklowitz, P. Böni, *Phys. Rev. Lett.* **2009**, *102*, 186602.
- [19] a) J. Fukuda, S. Zumer, *Phys. Rev. Lett.* **2011**, *106*, 097801; b) J. Fukuda, S. Zumer, *Nat. Commun.* **2011**, *2*, 246; c) J. Fukuda, M. Yoneya, H. Yokoyama, *Phys. Rev. E* **2009**, *80*, 031706.
- [20] U. K. Rößler, A. N. Bogdanov, C. Pfleiderer, *Nature* **2006**, *442*, 797–801.
- [21] Molecular structure optimization was performed by DFT with the uB97XD/6-31G(d) method using Gaussian09. The molecular lengths were assumed from the resulting dihedral angles around the ester, Schiff's base moieties, and alkoxy chains with all-*trans* zig-zag conformation.

Received: July 1, 2016

Published online: August 11, 2016